Faculty Bibliography 2000s | Faculty Bibliography

1-1-2004

Extended Cauchy equations for the refractive indices of liquid crystals

Jun Li
University of Central Florida

Shin-Tson Wu
University of Central Florida

Extended Cauchy equations for the refractive indices of liquid crystals

Jun Li, and Shin-Tson Wu

View Online   **Export Citation**

ARTICLES YOU MAY BE INTERESTED IN

Extended Cauchy equations for the refractive indices of liquid crystals

Jun Li and Shin-Tson Wu[a)]

School of Optics/CREOL, University of Central Florida, Orlando, Florida 32816

The extended Cauchy equations are derived based on the Vuks equation for describing the wavelength- and temperature-dependent refractive indices of liquid crystal compounds and mixtures. This model fits experimental data well in the off-resonance spectral region. Correlations between the Cauchy coefficients for the nematic and isotropic phases are derived and validated by experiments. © *2004 American Institute of Physics.* [DOI: 10.1063/1.1635971]

I. INTRODUCTION

Refractive indices of a liquid crystal (LC) are fundamentally interesting and practically useful parameters. Most liquid crystal light modulators, e.g., flat panel display devices, utilize the electric-field-induced refractive index change. In addition to the molecular constituents, the wavelength and temperature are the two most important factors affecting the LC refractive indices. For instance, to achieve a full-color display three primary colors [red, green, and blue (RGB)] are used. It is essential to know the wavelength-dependent refractive indices of the LC mixture employed in order to optimize the cell design. As the operating temperature changes, the refractive indices change accordingly. The temperature effect is particularly important for projection displays. Due to the thermal effect of the lamp, the temperature of the display panel could reach $50-60\,°C$. It is important to know the LC properties at the anticipated operating temperature beforehand.

Liquid crystal is a complex molecular system involving short and long range molecular interactions. Several models have attempted to address the wavelength and temperature dependencies of the LC refractive indices.[1–9] Each one has its own merits and demerits. The Vuks model[2] is analogous to the classical Clausius–Mossotti equation for correlating the microscopic LC molecular polarizability to the macroscopic refractive indices. However, the wavelength and temperature effects are not described explicitly. The single band model[4] gives an explicit expression on the wavelength and temperature dependence for birefringence, but not for the individual refractive indices. On the other hand, the three-band model[7] describes the origins of the LC refractive indices for single LC compounds. Unfortunately, the three-band model needs three fitting parameters for each LC compound. If a LC mixture consists of 5–10 distinct molecular structures, it would be too complicated for the three-band model to quantitatively describe the LC refractive indices of the mixture.

In this article, we derive the extended Cauchy equations for describing the wavelength- and temperature-dependent refractive indices of anisotropic liquid crystals. The original Cauchy equation was intended for the *isotropic* gases and

liquids.[10] The extended Cauchy equations not only apply to single compounds but also to LC mixtures. In Sec. II, we briefly discuss the pros and cons of the three-band model and show the derivation processes for the extended Cauchy equations. In Sec. III, we validate the extended Cauchy equations by experimental data. Excellent agreement between theory and experiment is obtained.

II. THEORY

In this section, we give analytical expressions of the three-band model and the extended Cauchy model and discuss their pros and cons.

A. Three-band model

In the three-band model,[7] one $\sigma \rightarrow \sigma^*$ transition (designated as the λ_0 band) and two $\pi \rightarrow \pi^*$ transitions (designated as the λ_1 and λ_2 bands with $\lambda_2 > \lambda_1$) are considered. The λ_0 band is located in the vacuum UV region ($\lambda_0 \sim 120$ nm), and λ_1 is located between 190 and 210 nm, not too sensitive to the LC structure, and λ_2 increases substantially as the molecular conjugation increases. For example, for the 4-cyano-4-*n*-pentyle-cyclohexane-phenyl (5PCH) LC compound, its $\lambda_1 = 200$ nm and $\lambda_2 = 235$ nm while for the 4-cyano-4-*n*-pentylbiphenyl (5CB) its λ_1 shifts to 210 nm and λ_2 shifts to 282 nm.[8] This is because 5CB has a longer molecular conjugation than 5PCH.

In the three-band model, the refractive indices (n_e and n_o) are expressed as follows:[7]

$$n_e \cong 1 + g_{0e}\frac{\lambda^2\lambda_0^2}{\lambda^2 - \lambda_0^2} + g_{1e}\frac{\lambda^2\lambda_1^2}{\lambda^2 - \lambda_1^2} + g_{2e}\frac{\lambda^2\lambda_2^2}{\lambda^2 - \lambda_2^2}, \quad (1a)$$

$$n_o \cong 1 + g_{0o}\frac{\lambda^2\lambda_0^2}{\lambda^2 - \lambda_0^2} + g_{1o}\frac{\lambda^2\lambda_1^2}{\lambda^2 - \lambda_1^2} + g_{2o}\frac{\lambda^2\lambda_2^2}{\lambda^2 - \lambda_2^2}. \quad (1b)$$

In the visible and infrared regions where $\lambda \gg \lambda_0$, the λ_0 band can be approximated by a constant and Eqs. (1a) and (1b) are simplified as

$$n_e \cong 1 + n_{0e} + g_{1e}\frac{\lambda^2\lambda_1^2}{\lambda^2 - \lambda_1^2} + g_{2e}\frac{\lambda^2\lambda_2^2}{\lambda^2 - \lambda_2^2}, \quad (2a)$$

$$n_o \cong 1 + n_{0o} + g_{1o}\frac{\lambda^2\lambda_1^2}{\lambda^2 - \lambda_1^2} + g_{2o}\frac{\lambda^2\lambda_2^2}{\lambda^2 - \lambda_2^2}. \quad (2b)$$

[a)]Electronic mail: swu@mail.ucf.edu

In Eq. (2), λ_1 and λ_2 could be determined from the ultraviolet absorption spectra of the compounds studied. The three unknowns are n_{0e}, g_{1e}, and g_{2e} for n_e and n_{0o}, g_{1o}, and g_{2o} for n_o. The major advantages of the three-band model are twofold: (1) it explains clearly the origins of the LC refractive indices, and (2) it allows quantitative assessment of each band's contribution to the overall refractive indices.[5] However, as shown in Eqs. (2a) and (2b) there are three unknowns involved in each index. For single LC compounds, this model works well. However, a LC mixture often consists of 5–10 components with different structures in order to lower the melting temperature and widen the nematic range. If each compound has its own three independent parameters, then a mixture would have too many unknowns. Thus, it is impractical for the three-band model to accurately describe the refractive indices of a complicated LC mixture unless the individual molecules all have similar core structures.

B. Extended Cauchy equations

The original Cauchy equation is intended for *isotropic* liquids and gases. Several authors have attempted to fit the refractive indices of *anisotropic* liquid crystals using Cauchy equations.[11,12] Although the fitting results are still satisfactory, the physical meaning is not clear.

In this section, we derive the extended Cauchy equations starting from the Vuks equation, which correlates the microscopic molecular polarizabilities ($\alpha_{e,o}$) of a liquid crystal to the macroscopic refractive indices:[2]

$$\frac{n_{e,o}^2 - 1}{\langle n^2 \rangle + 2} = \frac{4\pi}{3} N \alpha_{e,o}. \tag{3}$$

In Eq. (3), n_e and n_o are refractive indices for the extraordinary and ordinary rays, respectively, N is the number of molecules per unit volume, $\alpha_{e,o}$ is the molecular polarizability, and $\langle n^2 \rangle$ is the average value of the refractive indices defined as

$$\langle n^2 \rangle = (n_e^2 + 2n_o^2)/3. \tag{4}$$

In the Vuks equation, the local field effect is assumed to be isotropic. The Vuks equation provides some important physical insights for understanding the refractive indices of an anisotropic liquid crystal. However, its descriptions on the wavelength and temperature effects for n_e and n_o are not explicit.

By substituting Eq. (4) into Eq. (3) and separating n_e and n_o, we obtain

$$n_e = \left[1 + \frac{4\pi N \alpha_e}{1 - \frac{4}{9}\pi N(2\alpha_o + \alpha_e)} \right]^{1/2}, \tag{5a}$$

$$n_o = \left[1 + \frac{4\pi N \alpha_o}{1 - \frac{4}{9}\pi N(2\alpha_o + \alpha_e)} \right]^{1/2}. \tag{5b}$$

Equations (5a) and (5b) are very similar except for the different α. For most liquid crystals developed so far, their refractive indices are around 1.45–1.80. Therefore, the second term in the square root is larger than 1, but less than 2.24. In order to expand Eq. (5) into a power series, we rewrite Eq. (5a) as

$$n_e = \sqrt{2} \left[1 + \left(\frac{2\pi N \alpha_e}{1 - \frac{4}{9}\pi N(2\alpha_o + \alpha_e)} - \frac{1}{2} \right) \right]^{1/2}, \tag{6}$$

and then expand Eq. (6) into power series:

$$n_e \approx \frac{3\sqrt{2}}{4} + \frac{\sqrt{2}\pi N \alpha_e}{1 - \frac{4}{9}\pi N(2\alpha_o + \alpha_e)}. \tag{7a}$$

Similarly, n_o can be expanded as

$$n_o \approx \frac{3\sqrt{2}}{4} + \frac{\sqrt{2}\pi N \alpha_o}{1 - \frac{4}{9}\pi N(2\alpha_o + \alpha_e)}. \tag{7b}$$

From the above equations, the wavelength and temperature effects of LC refractive indices are determined by α_e and α_o. We need to find how α_e and α_o vary with wavelength and temperature.

Liquid crystal is a state of matter with physical properties lying between an isotropic liquid and a perfect crystal. Thus, its molecular differential polarizability $\alpha_e - \alpha_o$ is related to the crystalline state $\gamma_e - \gamma_o$ by the order parameter as[13]

$$\alpha_e - \alpha_o = S(\gamma_e - \gamma_0). \tag{8}$$

The average molecular polarizabilities $\langle \alpha \rangle$ and $\langle \gamma \rangle$ are related to their individual molecular polarizabilities as

$$\langle \alpha \rangle = \tfrac{1}{3}(2\alpha_0 + \alpha_e), \tag{9}$$

$$\langle \gamma \rangle = \tfrac{1}{3}(2\gamma_0 + \gamma_e). \tag{10}$$

Based on Eqs. (8)–(10), the individual molecular polarizabilities can be expressed as

$$\gamma_e = \langle \alpha \rangle + \frac{2(\alpha_e - \alpha_o)}{3S}, \tag{11}$$

$$\gamma_0 = \langle \alpha \rangle - \frac{\alpha_e - \alpha_o}{3S}, \tag{12}$$

$$\alpha_o = \langle \gamma \rangle - \frac{S}{3}(\gamma_e - \gamma_0), \tag{13}$$

$$\alpha_e = \langle \gamma \rangle + \frac{2S}{3}(\gamma_e - \gamma_0). \tag{14}$$

Substituting Eqs. (13) and (14) back to Eq. (9), we prove that:

$$\langle \gamma \rangle = \langle \alpha \rangle. \tag{15}$$

That means the average molecular polarizabilities in the liquid crystal state and crystalline state are essentially equal. Plug Eqs. (13)–(15) back to Eqs. (7a) and (7b), we obtain

$$n_e \approx \frac{3\sqrt{2}}{4} + \frac{\sqrt{2}\pi N\langle \alpha \rangle}{1 - \frac{4}{3}\pi N\langle \alpha \rangle} + \frac{\frac{2\sqrt{2}}{3}\pi NS(\gamma_e - \gamma_0)}{1 - \frac{4}{3}\pi N\langle \alpha \rangle}, \tag{16}$$

$$n_o \approx \frac{3\sqrt{2}}{4} + \frac{\sqrt{2}\,\pi N\langle\alpha\rangle}{1-\frac{4}{3}\pi N\langle\alpha\rangle} - \frac{\frac{\sqrt{2}}{3}\pi NS(\gamma_e-\gamma_0)}{1-\frac{4}{3}\pi N\langle\alpha\rangle}. \tag{17}$$

In Eqs. (16) and (17), the first term $3\sqrt{2}/4\sim 1.0607$ is close to unity, the second term is weakly dependent on temperature through the molecular packing density N and the average molecular polarizability $\langle\alpha\rangle$, and the third term is sensitive to the temperature as it depends on the order parameter. In a temperature not too close to the clearing temperature (T_c), the order parameter can be approximated as[14]

$$S=(1-T/T_c)^\beta, \tag{18}$$

where β is a material parameter; it depends on the LC molecular structure. In an isotropic state, $S=0$ and the third term vanish. Under such a circumstance, $n_e=n_o=n_i$ with

$$n_i(\lambda) \approx 1.0607 + \frac{\sqrt{2}\,\pi N\langle\alpha\rangle}{1-\frac{4}{3}\pi N\langle\alpha\rangle}. \tag{19}$$

For 5CB in the isotropic state, $n_i\sim 1.647$ at $\lambda=400$ nm and $n_i\sim 1.580$ at $\lambda=800$ nm.[7] From $\lambda=400$ to 800 nm, the refractive index is only decreased by $\sim 4\%$. That means in the isotropic state the refractive index is relatively insensitive to the wavelength. Substituting these numbers into Eq. (19), we find $0.247<\pi N\langle\alpha\rangle<0.267$, indicating that $\pi N\langle\alpha\rangle$ is not sensitive to the wavelength. This approximation should be applicable to other LC compounds as well. On the other hand, the temperature effect of n_i is through the packing density (N) variation, which is also very weak (for 5CB, $dn_i/dT\sim 4\times 10^{-4}$).

In the off-resonance region, the molecular polarizability ($\alpha_{e,o}$) is related to the electronic transition wavelength λ_i and the corresponding oscillator strength $(f_{e,o})_i$ as[15]

$$\alpha_{e,o}(\lambda) \approx \sum_i (f_{e,o})_i \frac{\lambda^2\lambda_i^2}{\lambda^2-\lambda_i^2}. \tag{20}$$

In Eq. (20), λ_i represents the three electronic transition bands involved. In the off-resonance region where $\lambda \gg \lambda_i$, the three bands can be merged to a single band with resonance wavelength λ^*:[4]

$$\gamma_{e,o} \propto Z f_{e,o}^* \frac{\lambda^2\lambda^{*2}}{\lambda^2-\lambda^{*2}}. \tag{21}$$

Thus, the differential molecular polarizability can be rewritten as

$$\gamma_e - \gamma_o = g Z(f_e^*-f_o^*)\frac{\lambda^2\lambda^{*2}}{\lambda^2-\lambda^{*2}}, \tag{22}$$

where g is a proportionality constant, Z is the number of active electrons per molecule, and (f^*) is the effective oscillator strength at the mean resonance wavelength λ^*. Substituting Eqs. (19) and (22) back to Eq. (16), we obtain

$$n_e(\lambda,T) \approx n_i(\lambda) + \frac{\frac{2\sqrt{2}}{3}\pi g N Z S(f_e^*-f_o^*)}{1-\frac{4}{3}\pi N\langle\alpha\rangle}\frac{\lambda^2\lambda^{*2}}{\lambda^2-\lambda^{*2}}. \tag{23}$$

As mentioned above, the $(4/3)\pi N\langle\alpha\rangle$ term in the denominator of Eq. (23) is insensitive to wavelength and temperature and, to the first order, can be treated as a constant. As a result, Eq. (23) can be further simplified as

$$n_e(\lambda,T) \approx n_i(\lambda) + GS\frac{\lambda^2\lambda^{*2}}{\lambda^2-\lambda^{*2}}. \tag{24a}$$

Similarly, n_o (and, hereafter, $\Delta n=n_e-n_o$) can be derived through the same process. Results are

$$n_o(\lambda,T) \approx n_i(\lambda) - \frac{GS}{2}\frac{\lambda^2\lambda^{*2}}{\lambda^2-\lambda^{*2}}, \tag{24b}$$

$$\Delta n(\lambda,T) \approx \frac{3GS}{2}\frac{\lambda^2\lambda^{*2}}{\lambda^2-\lambda^{*2}}, \tag{24c}$$

where

$$G=\frac{2\sqrt{2}}{3}\pi g N Z(f_e^*-f_o^*)\bigg/\left(1-\frac{4}{3}\pi N\langle\alpha\rangle\right),$$

is a proportionality constant.

The temperature effect of N and $f_e^*-f_o^*$ is much smaller than that of S. Thus, we can assume G is insensitive to the temperature. Equation (24c) is identical to the single-band birefringence dispersion model,[4] although the derivation procedures are not the same.

Although Eqs. (24a) and (24b) describe the wavelength and temperature effects of n_e and n_o, they still involve the isotropic state refractive index $n_i(\lambda)$. In the isotropic state, $n_i(\lambda)$ can be expressed by the traditional Cauchy equation:

$$n_i(\lambda)=A_i+\frac{B_i}{\lambda^2}+\frac{C_i}{\lambda^4}, \tag{25}$$

where A_i, B_i, and C_i are the Cauchy coefficients for the isotropic state.

Figure 1 shows the fitting of Eq. (25) to the experimental results of 5CB at $T=36.1\,°C$, which is above the clearing temperature (T_c) of 5CB ($T_c\sim 35.3\,°C$). Indeed, a very good fitting is obtained. The three Cauchy coefficients extracted are: $A_i=1.5721$, $B_i=0.0021\ \mu m^2$, and $C_i=0.0016\ \mu m^4$.

By substituting Eq. (25) into Eqs. (24a) and (24b), we obtain:

$$n_e=A_i+\frac{B_i}{\lambda^2}+\frac{C_i}{\lambda^4}+GS\frac{\lambda^2\lambda^{*2}}{\lambda^2-\lambda^{*2}}, \tag{26a}$$

$$n_o=A_i+\frac{B_i}{\lambda^2}+\frac{C_i}{\lambda^4}-\frac{GS}{2}\frac{\lambda^2\lambda^{*2}}{\lambda^2-\lambda^{*2}}. \tag{26b}$$

In the off-resonance region where ($\lambda \gg \lambda^*$), we can expand the right-hand terms of Eqs. (26a) and (26b) into a power series. Retaining the λ^{-2} and λ^{-4} terms, we derive the following extended Cauchy equations:
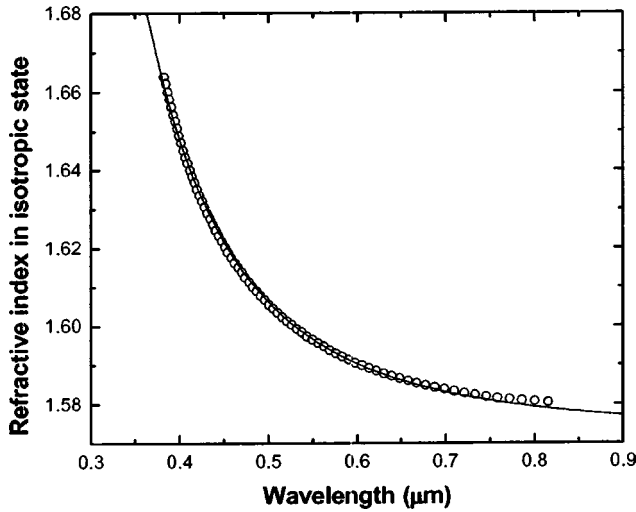
FIG. 1. Wavelength-dependent refractive index of 5CB in an isotropic state, $T = 36.1\,°C$. Circles are experimental data and solid lines are fittings using Eq. (25). The fitting parameters are: $A_i = 1.5721$, $B_i = 0.0021\ \mu m^2$, and $C_i = 0.0016\ \mu m^4$.

FIG. 2. Wavelength-dependent refractive indices of 5CB at $T = 25.1\,°C$. Open and closed circles are experimental data for n_e and n_o, respectively. Solid line represents the three-band model and dashed lines are for the extended Cauchy model. The fitting parameters are listed in Table I.

$$n_e = A_e + \frac{B_e}{\lambda^2} + \frac{C_e}{\lambda^4}, \tag{27a}$$

$$A_e = A_i + A'_e S, \tag{27b}$$

$$B_e = B_i + B'_e S, \tag{27c}$$

$$C_e = C_i + C'_e S, \tag{27d}$$

where $A'_e = G\lambda^{*2}$, $B'_e = G\lambda^{*4}$, $C'_e = G\lambda^{*6}$, and A_i, B_i, and C_i are the Cauchy coefficients of the LC in its isotropic state. By the same procedures, we find the Cauchy coefficients for n_o:

$$n_o = A_o + \frac{B_o}{\lambda^2} + \frac{C_o}{\lambda^4} \tag{28a}$$

$$A_o = A_i - A'_o S, \tag{28b}$$

$$B_o = B_i - B'_o S, \tag{28c}$$

$$C_o = C_i - C'_o S, \tag{28d}$$

where $A'_o = G\lambda^{*2}/2$, $B'_o = G\lambda^{*4}/2$, and $C'_o = G\lambda^{*6}/2$.

Equations (27) and (28) give the complete temperature and wavelength dependence of the liquid crystal refractive indices. Equations (27) and (28) can be applied to LC mixtures as well. The n_e and n_o of each compound in the mixture share the same forms as Eqs. (27a) and (28a) except for the different Cauchy coefficients. These individual equations can be superimposed and still lead to the same Cauchy form. Thus, the extended Cauchy equations can be applied to single compounds and mixtures.

As shown in Eqs. (27a) and (28a), at a given temperature both n_e and n_o decrease as the wavelength increases. In the long wavelength region ($\lambda > 1\ \mu m$), the contributions of the B and C terms become negligible. Under these conditions, $n_e \rightarrow A_e$ and $n_o \rightarrow A_o$; they are independent of wavelength. This result is consistent with many experimental evidences.
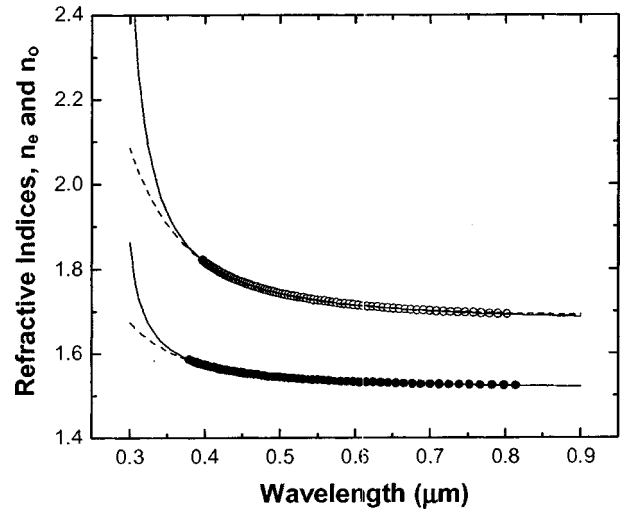
Equations (27) and (28) predict that if we plot the Cauchy coefficients as a function of the order parameter, straight lines with positive slopes for n_e and negative slopes for n_o should be found. Moreover, each corresponding parameter for n_e and n_o (e.g., A_e and A_o) will intersect at $S = 0$, and the intersections are A_i, B_i, and C_i; the Cauchy's coefficients in the isotropic phase.

III. RESULTS AND DISCUSSIONS

The extended Cauchy model we derive here has three fitting parameters. To validate this model, we need to have at least half a dozen data points. From the literature, we found that 5CB has the most complete experimental refractive index data.[7] At a given temperature, there are more than 50 refractive index data measured spanning in the 400–800 nm spectral range.

A. Comparisons of models

Figure 2 depicts the fittings of the experimental data of 5CB using the three-band model (solid lines) and the extended Cauchy equations (dashed lines). The fitting parameters are listed in Table I. In the visible and near-infrared regions, both models give excellent fits to the experimental data. In the UV region, the deviation between these two models becomes more apparent. The three-band model con-

TABLE I. Fitting parameters for the three-band model and the extended Cauchy equations. LC: 5CB at $T = 25.1\,°C$. The units of Cauchy's B and C coefficients are μm^2 and μm^4, respectively.

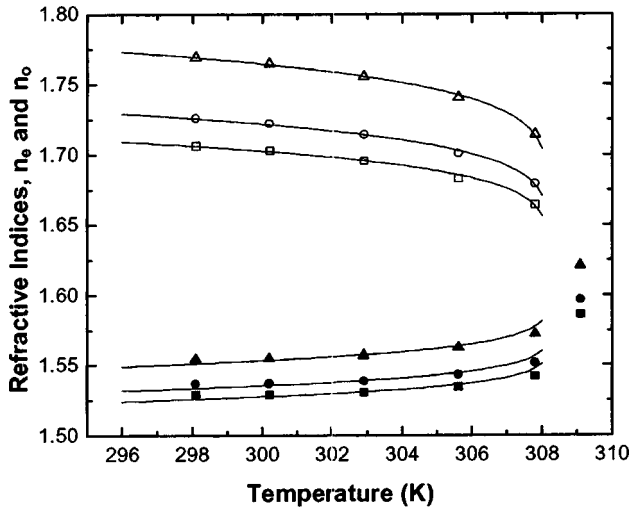| Model	n_e			n_o		
Three-band model	n_{0e} 0.4618	g_{1e} 2.1042	g_{2e} 1.4413	n_{0o} 0.4202	g_{1o} 1.2286	g_{2o} 0.4934
Cauchy model	A_e 1.6795	B_e 0.0048	C_e 0.0027	A_o 1.5187	B_o 0.0016	C_o 0.0011

FIG. 3. Temperature-dependent refractive indices of 5CB. Open and filled triangles, circles, and squares are experimental data for n_e and n_o at λ = 450, 550, and 650 nm, respectively. Measurement temperatures are 25.1, 27.2, 29.9, 32.6, 34.8, and 36.1 °C. T_c = 35.3 °C. Solid lines are fitting curves using Eqs. (29a) and (29b).

siders the resonance effect, but the extended Cauchy model does not. Thus, in the near-resonance region the results from the three-band model are more accurate.

B. Temperature effect

From Eqs. (24a) and (24b), at a given wavelength, the refractive indices have the following forms:

$$n_e(T) \approx n_i + G'\left(1 - \frac{T}{T_c}\right)^{\beta},$$ (29a)

$$n_o(T) \approx n_i - \frac{G'}{2}\left(1 - \frac{T}{T_c}\right)^{\beta},$$ (29b)

where n_i is the refractive index in the isotropic state and $G' = G[\lambda^2\lambda^{*2}/(\lambda^2 - \lambda^{*2})]$ and β are fitting parameters. For 5CB, the experimental refractive index data at T = 25.1, 27.2, 29.9, 32.6, 34.8, and 36.1 °C are available in the λ = 400–800 nm range. To illustrate the calculation methods, we selected the data at three primary colors (λ = 450, 550, and 650 nm) used for display applications.

Figure 3 plots the temperature-dependent refractive indices of 5CB at λ = 450 (triangles), 550 (circles), and 650 nm (squares). The solid lines are fitting curves using parameters listed in Table II. The fitting results are quite satisfactory. As

TABLE II. Parameters obtained by fitting temperature-dependent n_e and n_o data of 5CB using Eqs. (29a) and (29b).

λ (nm)	n_i	n_e		n_o	
		G'	β	G'	β
450	1.6209	0.2440	0.1461	0.2298	0.1461
550	1.5965	0.2092	0.1414	0.2042	0.1414
650	1.5865	0.1914	0.1375	0.1942	0.1375

the temperature increases, n_e decreases gradually while n_o increases slightly. At a given temperature, both n_e and n_o increase as the wavelength decreases.

It is noteworthy that Eqs. (29a) and (29b) are interrelated. Although each equation has two adjustable parameters (G' and β; provided that n_i is known), these two parameters have to fit both n_e and n_o simultaneously. During the fitting process, we first obtained G' and β for each wavelength by fitting the temperature-dependent n_e of 5CB using Eq. (29a). We then fixed the β value and fitted the n_o data through Eq. (29b) by only using G' as a variable parameter. For the RGB wavelengths studied, the obtained G' values for n_e and n_o agree within 5%. From Table II, G' decreases as the wavelength increases. The same trend holds for both n_e and n_o. In principle, the β exponent should not depend on the wavelength employed. From Table II, we find $\beta = 0.142 \pm 0.004$, the variation is within $\pm 3\%$.

C. Correlations between Cauchy coefficients

According to Eqs. (27) and (28), the Cauchy coefficients for both n_e and n_o are linearly proportional to the order parameter (S). If we plot the Cauchy coefficients as a function of S, then straight lines with positive and negative slopes for n_e and n_o, respectively, should be obtained. The interceptions at $S = 0$ lead to the Cauchy coefficients at the isotropic state.

To validate these predictions, we used the experimental data of 5CB. The order parameter described in Eq. (18) is determined by the clearing temperature T_c and β exponent. The clearing temperature of 5CB is 308.3 K. Therefore, by fitting the temperature-dependent birefringence data at a given wavelength we can obtain β easily. The β value we found is 0.142 (as listed in Table II). Using this β value, we can calculate the order parameter at the specific measurement temperatures. In the mean time, by fitting the experimental data for n_e and n_o using the extended Cauchy equations, we

TABLE III. Cauchy coefficients and order parameters of 5CB. T_c = 308.3 K and β = 0.142.

| T (K)	T/T_c	S	A_e	B_e	C_e	A_o	B_o	C_o
298.1	0.967 23	0.615 46	1.679 46	0.004 82	0.002 73	1.518 66	0.001 63	0.001 14
300.2	0.974 04	0.595 42	1.676 49	0.004 89	0.002 66	1.518 64	0.001 63	0.001 16
302.9	0.982 80	0.561 61	1.670 30	0.004 62	0.002 57	1.520 12	0.001 58	0.001 21
305.6	0.991 56	0.507 594	1.658 66	0.004 40	0.002 48	1.523 69	0.001 74	0.001 25
307.8	0.998 70	0.389 115	1.643 04	0.003 80	0.002 17	1.530 28	0.001 83	0.001 35
309.1	1.002 92	0	1.572 09	0.002 10	0.001 61	1.572 09	0.002 10	0.001 61
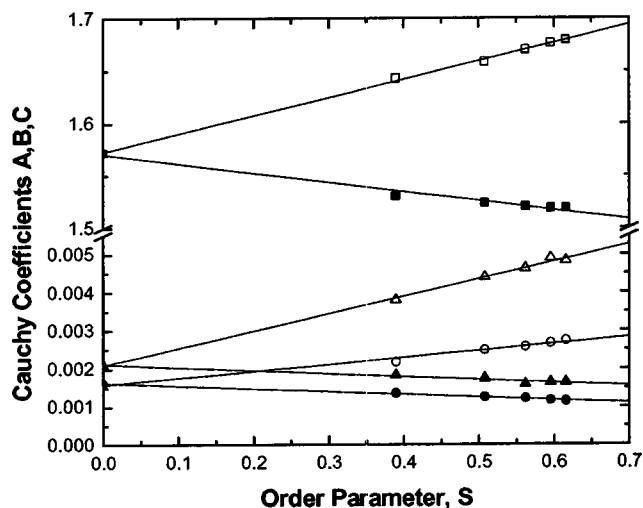
FIG. 4. Order parameter dependent Cauchy coefficients. Squares, triangles, and circles are the *ABC* Cauchy coefficients obtained by fitting the 5CB data at six different temperatures. Open and filled squares, triangles, and circles are for $[A_e,A_o]$ $[B_e,B_o]$, and $[C_e,C_o]$, respectively. Solid lines are fitting results.

could extract the corresponding Cauchy coefficients. The results are listed in Table III.

Figure 4 shows the order parameter dependent Cauchy coefficients $A_{e,o}$ (squares), $B_{e,o}$ (triangles), and $C_{e,o}$ (circles) for 5CB. Indeed, straight lines are found. The A_e, B_e, and C_e coefficients have positive slopes while A_o, B_o, and C_o have negative slopes. The slope (A'_e, A'_o, etc.) of each line is listed in Tables IV for n_e and n_o, respectively. The corresponding line pairs (A_e,A_o), (B_e,B_o), and (C_e,C_o) intersect at $S=0$. The interceptions agree quite well with the Cauchy coefficients A_i, B_i, and C_i obtained from the isotropic phase.

Based on the Cauchy coefficients listed in Table IV, the birefringence of 5CB can be calculated at any desired wavelength and temperature. This feature is particularly important for the elevated temperature operation of liquid crystal devices.

IV. CONCLUSIONS

We have developed extended Cauchy equations for describing the wavelength- and temperature-dependent refractive indices of liquid crystal compounds and mixtures. The model fits well with the experimental results of 5CB. This model is particularly useful for fitting the experimental data of liquid crystal mixtures where the three-band model fails. However, in the near-resonance region, the extended Cauchy model has less accuracy than that of the three-band model.

TABLE IV. Parameters $A'_{e,o}$, $B'_{e,o}$, $C'_{e,o}$, A_i, B_i, and C_i obtained from the slopes and interceptions in Fig. 4.

5CB	Cauchy coefficients					
n_e	A'_e	A_i	B'_e	B_i	C'_e	C_i
	0.1738	1.5721	0.0045	0.0021	0.0018	0.0016
n_o	A'_o	A_i	B'_o	B_i	C'_o	C_i
	0.0885	1.5721	0.0008	0.0021	0.0007	0.0016

[1] H. E. Neugebauer, Can. J. Phys. **32**, 1 (1954).
[2] M. F. Vuks, Opt. Spektrosk. **20**, 644 (1966).
[3] W. H. de Jeu, *Physical Properties of Liquid Crystalline Materials* (Gordon and Breach, New York, 1980), Chap. 4.
[4] S. T. Wu, Phys. Rev. A **33**, 1270 (1986).
[5] S. T. Wu, J. Appl. Phys. **69**, 2080 (1991).
[6] I. Abdulhalim, Mol. Cryst. Liq. Cryst. **197**, 103 (1991).
[7] S. T. Wu, C. S. Wu, M. Warenghem, and M. Ismaili, Opt. Eng. (Bellingham) **32**, 1775 (1993).
[8] I. C. Khoo and S. T. Wu, *Optics and Nonlinear Optics of Liquid Crystals* (World Scientific, Singapore, 1993).
[9] E. M. Averyanov, J. Opt. Technol. **64**, 417 (1997).
[10] M. Born and E. Wolf, *Principle of Optics*, 6th ed. (Pergamon, New York, 1980).
[11] H. Mada and S. Kobayashi, Mol. Cryst. Liq. Cryst. **33**, 47 (1976).
[12] L. Pohl and U. Finkenzeller, in *Liquid Crystals: Applications and Uses*, edited by B. Bahadur (World Scientific, Singapore, 1990), Vol. 1, Chap. 4.
[13] L. M. Blinov, *Electro-Optical and Magneto-Optical Properties of Liquid Crystals* (Wiley, New York, 1983), Chap. 2.
[14] I. Haller, Prog. Solid State Chem. **10**, 103 (1975).
[15] A. D. Buckingham, in *Molecular Electro-Optics*, edited by C. T. O'Konski (Dekker, New York, 1976), Chap. 2.